MODAL LOCALIZATION IN VIBRATING CIRCULAR CYLINDRICAL SHELLS

Francesco Pellicano, Antonio Zippo and Marco Barbieri

University of Modena and Reggio Emilia, Department of Engineering "Enzo Ferrari", Modena, Italy
email: francesco.pellicano@unimore.it

Matteo Strozzi

University of Ferrara, Department of Engineering, Ferrara, Italy

The goal of the present paper is the analysis of the effect of geometric imperfections in circular cylindrical shells. Perfect circular shells are characterized by the presence of double shell-like modes, i.e., modes having the same frequency with modal shape shifted of a quarter of wavelength in the circumferential direction. In presence of geometric imperfections, the double natural frequencies split into a pair of distinct frequencies, the splitting is proportional to the level of imperfection. In some cases, the imperfections cause an interesting phenomenon on the modal shapes, which present a strong localization in the circumferential direction. This study is carried out by means of a semi-analytical approach compared with standard finite element analyses.
Keywords: modal localization, circular cylindrical shells

1. Introduction

Circular cylindrical shells have been proven to be sensitive to initial geometric imperfections.

Kubenko and Koval'chuk [1] reviewed many studies on the influence of the initial imperfections on the natural frequencies and mode shapes of elastic shells. They analysed the splitting of the natural frequencies of two conjugate modes as a measure of the initial geometric imperfections imposed.

Katawala and Nash [2] studied the influence of the initial geometric imperfections on the vibrations of thin circular cylindrical shells. They found that the natural frequency of free vibration of the imperfect modes increases with increasing the amplitude of imperfection on the modal shape.

Shen and Li [3] studied the dynamic behaviour of shear deformable laminated cylindrical shells subjected to combined axial compression and uniform temperature loading. They evaluated the effect of the modal geometric imperfections on the buckling and post-buckling deformations.

Other relevant studies on the influence of the initial geometric imperfections on the vibrations of circular cylindrical shell can be found in Refs. [4-5].

In the present paper, the linear vibrations and modal localization in circular cylindrical shells are analysed in the framework of the Sanders-Koiter theory [6-8]. The shell deformation is described in terms of longitudinal, circumferential and radial displacement fields. Clamped-clamped boundary conditions are investigated. The three displacement fields are expanded by means of a double mixed series based on Chebyshev polynomials for the longitudinal variable and harmonic functions for the circumferential variable; the Rayleigh-Ritz method is used to get approximated natural frequencies (eigenvalues) and mode shapes (eigenfunctions). The three displacement fields are re-expanded by using the previous approximated eigenfunctions [9-12]; conjugate mode shapes are used; geometric imperfections are imposed on the modes in order to investigate the modal localization of the shells.

The semi-analytical approach proposed in the paper is validated in linear field by means of comparisons with finite element analyses.

2. Sanders-Koiter linear shell theory

In Figure 1, a circular cylindrical shell having radius R, length L and thickness h is represented; a cylindrical coordinate system $(0;\ x,\ \theta,\ z)$ is considered to take advantage from the axial symmetry; the origin 0 of the reference system is located at the centre of one end of the shell. Three displacement fields are represented: longitudinal $u\ (x,\ \theta,\ t)$, circumferential $v\ (x,\ \theta,\ t)$ and radial $w\ (x,\ \theta,\ t)$.

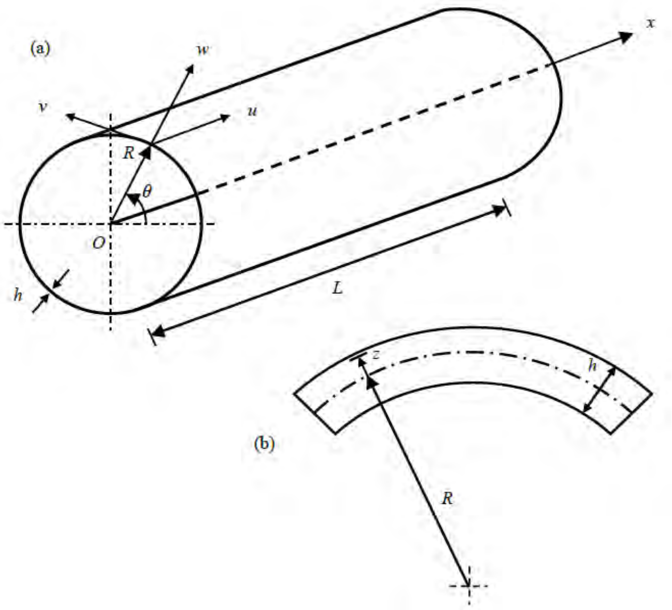

Figure 1: Geometry of the functionally graded shell. (a) Complete shell; (b) cross-section of the shell surface.

2.1 Strain-displacement relationships

The Sanders-Koiter shell theory is based on the Love's first approximation [6]. The strain components $(\varepsilon_x,\ \varepsilon_\theta,\ \gamma_{x\theta})$ are related to the middle surface strains $(\varepsilon_{x,0},\ \varepsilon_{\theta,0},\ \gamma_{x\theta,0})$ and to the changes in curvature and torsion $(k_x,\ k_\theta,\ k_{x\theta})$ of the middle surface of the shell by the following relationships [6]

$$\varepsilon_x = \varepsilon_{x,0} + z k_x \qquad \varepsilon_\theta = \varepsilon_{\theta,0} + z k_\theta \qquad \gamma_{x\theta} = \gamma_{x\theta,0} + z k_{x\theta} \tag{1}$$

where z is the distance of an arbitrary point of the shell from the shell middle surface and $(x,\ \theta)$ are the longitudinal and angular coordinates of the shell, see Figure 1.

The middle surface strains and changes in curvature and torsion of the shell are given by [6]

$$\begin{gathered}
\varepsilon_{x,0} = \frac{1}{L}\frac{\partial u}{\partial \eta} + \frac{1}{L^2}\frac{\partial w}{\partial \eta}\frac{\partial w_0}{\partial \eta} \qquad \varepsilon_{\theta,0} = \frac{w}{R} + \frac{1}{R}\frac{\partial v}{\partial \theta} + \frac{1}{R^2}\left(\frac{\partial w}{\partial \theta} - v\right)\frac{\partial w_0}{\partial \theta} \\
\gamma_{x\theta,0} = \frac{1}{R}\frac{\partial u}{\partial \theta} + \frac{1}{L}\frac{\partial v}{\partial \eta} + \frac{1}{LR}\frac{\partial w}{\partial \eta}\frac{\partial w_0}{\partial \theta} + \frac{1}{LR}\left(\frac{\partial w}{\partial \theta} - v\right)\frac{\partial w_0}{\partial \eta} \\
k_x = -\frac{1}{L^2}\frac{\partial^2 w}{\partial \eta^2} \qquad k_\theta = \frac{1}{R^2}\left(\frac{\partial v}{\partial \theta} - \frac{\partial^2 w}{\partial \theta^2}\right) \qquad k_{x\theta} = -\frac{2}{LR}\frac{\partial^2 w}{\partial \eta \partial \theta} + \frac{1}{2R}\left(\frac{3}{L}\frac{\partial v}{\partial \eta} - \frac{1}{R}\frac{\partial u}{\partial \theta}\right)
\end{gathered} \tag{2}$$

where $(\eta = x / L)$ is the nondimensional longitudinal coordinate and w_0 is a geometric imperfection.

In the case of isotropic cylindrical shell, the stresses are related to the strains as follows [6]

$$\sigma_x = \frac{E}{1-\nu^2}(\varepsilon_x + \nu\varepsilon_\theta) \qquad \sigma_\theta = \frac{E}{1-\nu^2}(\varepsilon_\theta + \nu\varepsilon_x) \qquad \tau_{x\theta} = \frac{E}{2(1+\nu)}\gamma_{x\theta} \tag{3}$$

where E is the Young's modulus and ν the Poisson's ratio. The plane stress hypothesis gives $\sigma_z = 0$.

2.2 Elastic strain energy and kinetic energy

The elastic strain energy of a cylindrical shell is given by [6]

$$U_s = \frac{1}{2} LR \int_0^1 \int_0^{2\pi} \int_{-h/2}^{h/2} (\sigma_x \varepsilon_x + \sigma_\theta \varepsilon_\theta + \tau_{x\theta} \gamma_{x\theta}) d\eta d\theta dz \tag{4}$$

where h, R and L are the thickness, radius and length of the shell, respectively.

The kinetic energy of a cylindrical shell (rotary inertia effect being neglected) is given by [6]

$$T_s = \frac{1}{2} \rho h LR \int_0^1 \int_0^{2\pi} (\dot{u}^2 + \dot{v}^2 + \dot{w}^2) \, d\eta \, d\theta \tag{5}$$

where ρ is the mass density of the shell.

3. Discretization approach

In order to carry out the linear analysis of the shell, a two-step procedure is applied [9]: i) the three displacement fields are expanded using a double mixed series and the Rayleigh-Ritz method is applied to obtain approximated eigenfunctions; ii) the displacement fields are re-expanded by using the approximated eigenfunctions and geometric imperfections are imposed on the modes.

3.1 First expansion

A modal vibration, i.e., a synchronous motion, can be formally written in the form [9]

$$u(\eta,\theta,t) = U(\eta,\theta) f(t) \qquad v(\eta,\theta,t) = V(\eta,\theta) f(t) \qquad w(\eta,\theta,t) = W(\eta,\theta) f(t) \tag{6}$$

where (u,v,w) are the three displacement fields, (U,V,W) denote the mode shape and $f(t)$ describes the time law, which is supposed to be the same for each displacement field (synchronous motion).

The mode shape is expanded by means of a double mixed series: harmonic functions along the circumferential direction, Chebyshev orthogonal polynomials along the longitudinal direction [9]

$$U(\eta,\theta) = \sum_{m=0}^{M_u} \sum_{n=0}^{N} \tilde{U}_{m,n} T_m^*(\eta) \cos n\theta \qquad V(\eta,\theta) = \sum_{m=0}^{M_v} \sum_{n=0}^{N} \tilde{V}_{m,n} T_m^*(\eta) \sin n\theta$$
$$W(\eta,\theta) = \sum_{m=0}^{M_w} \sum_{n=0}^{N} \tilde{W}_{m,n} T_m^*(\eta) \cos n\theta \tag{7}$$

where $T_m^*(\eta) = T_m(2\eta - 1)$, m is the degree of the Chebyshev polynomials, n is the number of nodal diameters and $(\tilde{U}_{m,n}, \tilde{V}_{m,n}, \tilde{W}_{m,n})$ are the generalized coordinates.

Clamped-clamped boundary conditions are imposed by applying constraints to the coefficients $(\tilde{U}_{m,n}, \tilde{V}_{m,n}, \tilde{W}_{m,n})$ of expansions (7) in the form [9]

$$u = 0 \qquad v = 0 \qquad w = 0 \qquad w_{,\eta} = 0 \qquad \text{for } \eta = 0,1 \tag{8}$$

Equations (6) are inserted into the expressions of U_s and T_s (equations (4-5)).

After imposing the stationarity to the Rayleigh quotient, one obtains the eigenvalue problem [9]

$$(-\omega^2 M + K)\tilde{q} = 0 \tag{9}$$

which furnishes natural frequencies and modes of vibration (eigenvalues and eigenvectors).

3.2 Modal re-expansion

In the modal re-expansion, the displacement fields (u,v,w) are expanded by using the linear mode shapes (U,V,W) obtained in the previous analysis and the conjugate mode shapes (U_c,V_c,W_c) [6]

$$\begin{aligned} u(\eta,\theta,t) &= \sum_{j=1}^{N_u}\sum_{n=1}^{N}\left[U^{(j,n)}(\eta,\theta)f_{u,j,n}(t)+U_c^{(j,n)}(\eta,\theta)f_{u,j,n,c}(t)\right] \\ v(\eta,\theta,t) &= \sum_{j=1}^{N_v}\sum_{n=1}^{N}\left[V^{(j,n)}(\eta,\theta)f_{v,j,n}(t)+V_c^{(j,n)}(\eta,\theta)f_{v,j,n,c}(t)\right] \\ w(\eta,\theta,t) &= \sum_{j=1}^{N_w}\sum_{n=1}^{N}\left[W^{(j,n)}(\eta,\theta)f_{w,j,n}(t)+W_c^{(j,n)}(\eta,\theta)f_{w,j,n,c}(t)\right] \end{aligned} \tag{10}$$

These expansions respect exactly the clamped-clamped boundary conditions; the synchronicity is relaxed since for each mode j and each component (u,v,w) different time laws are allowed.

The mode shapes ($U^{(j,n)}$,$V^{(j,n)}$,$W^{(j,n)}$) are known functions expressed in terms of polynomials and harmonic functions, see equations (7); the index n indicates the number of nodal diameters, the index j is used for ordering the modes (for each n) with increasing associated natural frequency.

The geometric imperfections w_0 are taken into account in the modal re-expansions (10).

Conjugate mode shapes can be straightforwardly obtained from expansions (7) [6]

$$\begin{aligned} U_c^{(j,n)}(\eta,\theta) &= \sum_{m=0}^{M_u}\sum_{n=1}^{N}\tilde{U}_{m,n}^{(j)}T_m^*(\eta)\sin n\theta \qquad V_c^{(j,n)}(\eta,\theta) = \sum_{m=0}^{M_v}\sum_{n=1}^{N}\tilde{V}_{m,n}^{(j)}T_m^*(\eta)\cos n\theta \\ W_c^{(j,n)}(\eta,\theta) &= \sum_{m=0}^{M_w}\sum_{n=1}^{N}\tilde{W}_{m,n}^{(j)}T_m^*(\eta)\sin n\theta \end{aligned} \tag{11}$$

It is to be noted that axisymmetric modes (n=0) do not exhibit any conjugate mode.

Equations (10) are then inserted into expressions of U_s and T_s (equations (4-5)).

After imposing the stationarity to the Rayleigh quotient, one obtains the eigenvalue problem (9), which gives natural frequencies, modes of vibration and modal shapes (eigenfunctions).

4. Numerical results

The mechanical properties of the circular cylindrical shell considered are reported in Table 1.

Table 1: Mechanical parameters of the clamped-clamped circular cylindrical shell.

Young's modulus E [GPa]	27.58
Poisson's ratio v	0.42
Mass density ρ [kg/m^3]	1541
Thickness h [mm]	0.25
Radius R [mm]	43.65
Length L [mm]	95.50

4.1 Validation of the semi-analytical approach

In order to validate the semi-analytical approach proposed in this paper, the natural frequencies of the clamped-clamped cylindrical shell of Table 1 obtained by applying the Sanders-Koiter theory are compared with those obtained by FE analyses, see Table 2. These comparisons show that the present semi-analytical method gives results close to the FEM, the differences being less than 2%.

Table 2: Natural frequencies of the clamped-clamped circular cylindrical shell of Table 1. Comparisons between Sanders-Koiter shell theory (SKT) and finite element method (FEM).

Mode	Natural frequency (Hz)		Difference %
(j,n)	SKT	FEM	
(1,7)	1850.49	1834.56	0.86
(1,6)	1850.97	1828.80	1.20
(1,12)	4099.48	4087.13	0.30
(3,7)	4997.47	4950.22	0.95
(3,12)	5056.77	5026.58	0.60
(1,14)	5543.33	5525.31	0.33
(3,6)	5761.41	5699.60	1.07
(3,14)	6262.87	6226.28	0.58
(1,0)	15303.9	15315.8	0.08
(3,0)	15478.3	15783.9	1.97
(5,0)	15972.0	16286.4	1.97

4.2 Effect of the geometric imperfections on the modal localization

In the modal re-expansions (10), the following modes are considered:

- (1,7), (1,7,*c*), (1,6), (1,6,*c*), (1,12), (1,12,*c*), (3,7), (3,7,*c*), (1,14), (1,14,*c*), (3,6), (3,6,*c*), (1,0), (3,0), (5,0) along the longitudinal field u
- (1,7), (1,7,*c*), (1,6), (1,6,*c*), (1,12), (1,12,*c*), (3,7), (3,7,*c*), (3,12), (3,12,*c*), (1,14), (1,14,*c*), (3,6), (3,6,*c*), (3,14), (3,14,*c*) along the circumferential field v
- (1,7), (1,7,*c*), (1,6), (1,6,*c*), (1,12), (1,12,*c*), (3,7), (3,7,*c*), (1,14), (1,14,*c*), (3,6), (3,6,*c*), (1,0), (3,0), (5,0) along the radial field w

and the maximum number of degrees of freedom of the system is equal to (N_{max} = 46).

The asymmetric geometric imperfections (initial radial displacement field w_0) are imposed on the modes (1,7), (1,7,*c*), (1,6), (1,6,*c*) in the following form

$$w_0(\eta,\theta) = wp_{(1,7)}W^{(1,7)}(\eta,\theta) + wp_{(1,7,c)}W_c^{(1,7)}(\eta,\theta) + wp_{(1,6)}W^{(1,6)}(\eta,\theta) + wp_{(1,6,c)}W_c^{(1,6)}(\eta,\theta) \tag{12}$$

where $W^{(j,n)}$ are the radial mode shapes of the modes and $wp_{(j,n)}$ are the initial geometric imperfections imposed on the modes along the radial direction.

In Figures 2-5 different values of initial geometric imperfections are imposed on the modes (1,7), (1,7,*c*), (1,6), (1,6,*c*) to investigate the localization of the modal shapes in the circumferential direction. The results of the Sanders-Koiter shell theory are compared with finite element analyses.

In Figure 2, the initial imperfections applied are $wp_{(1,6)} = wp_{(1,6,c)} = 0.2h$, $wp_{(1,7)} = wp_{(1,7,c)} = 0$: the same initial imperfection imposed on the conjugate modes (1,6), (1,6,*c*) gives no modal localization on all the considered modes.

In Figure 3, the initial imperfections used are $wp_{(1,6)} = 0.4h$, $wp_{(1,6,c)} = 0.2h$, $wp_{(1,7)} = wp_{(1,7,c)} = 0$: different initial imperfections imposed on the conjugate modes (1,6), (1,6,*c*) give no modal localization on all the considered modes.

Therefore, from Figures 2-3, it can be observed that any initial geometric imperfection imposed on two conjugate modes gives no localization on the modal shape of all the modes.

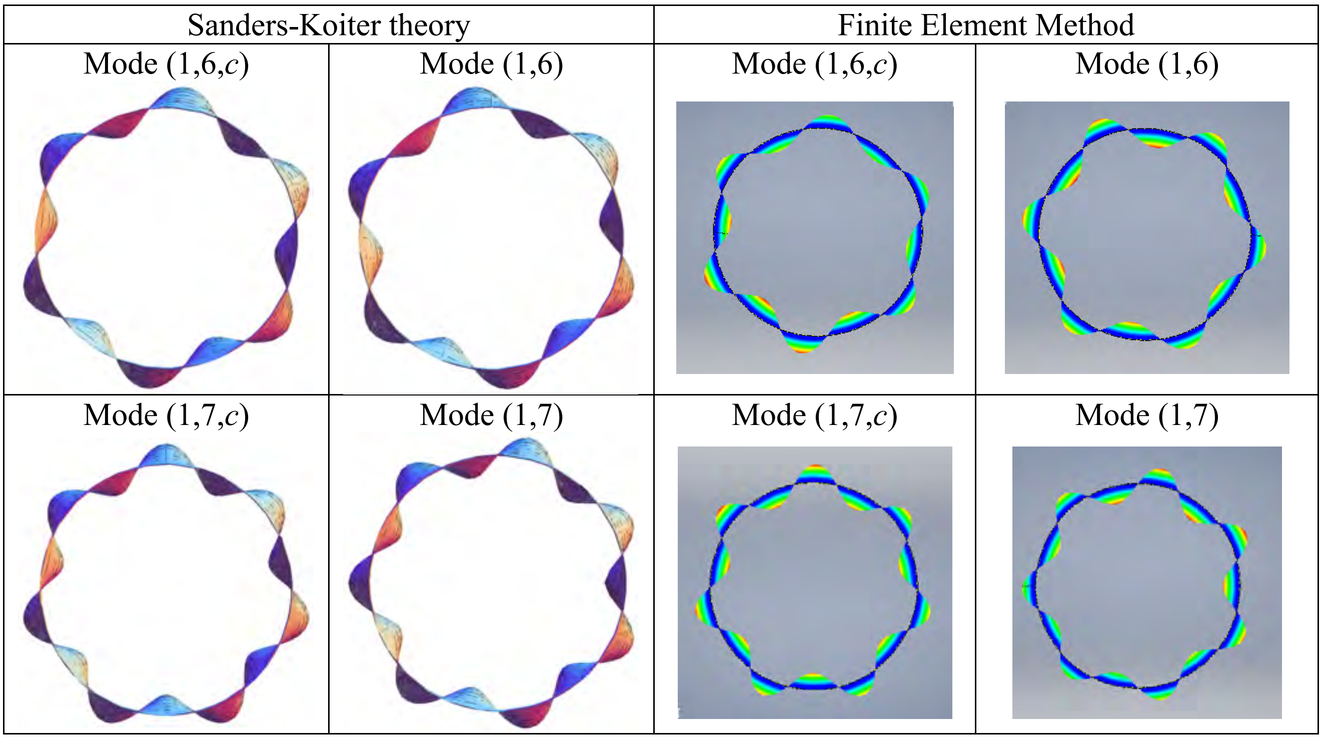

Figure 2: Initial geometric imperfections $wp_{(1,6)} = wp_{(1,6,c)} = 0.2h$, $wp_{(1,7)} = wp_{(1,7,c)} = 0$. No localization.

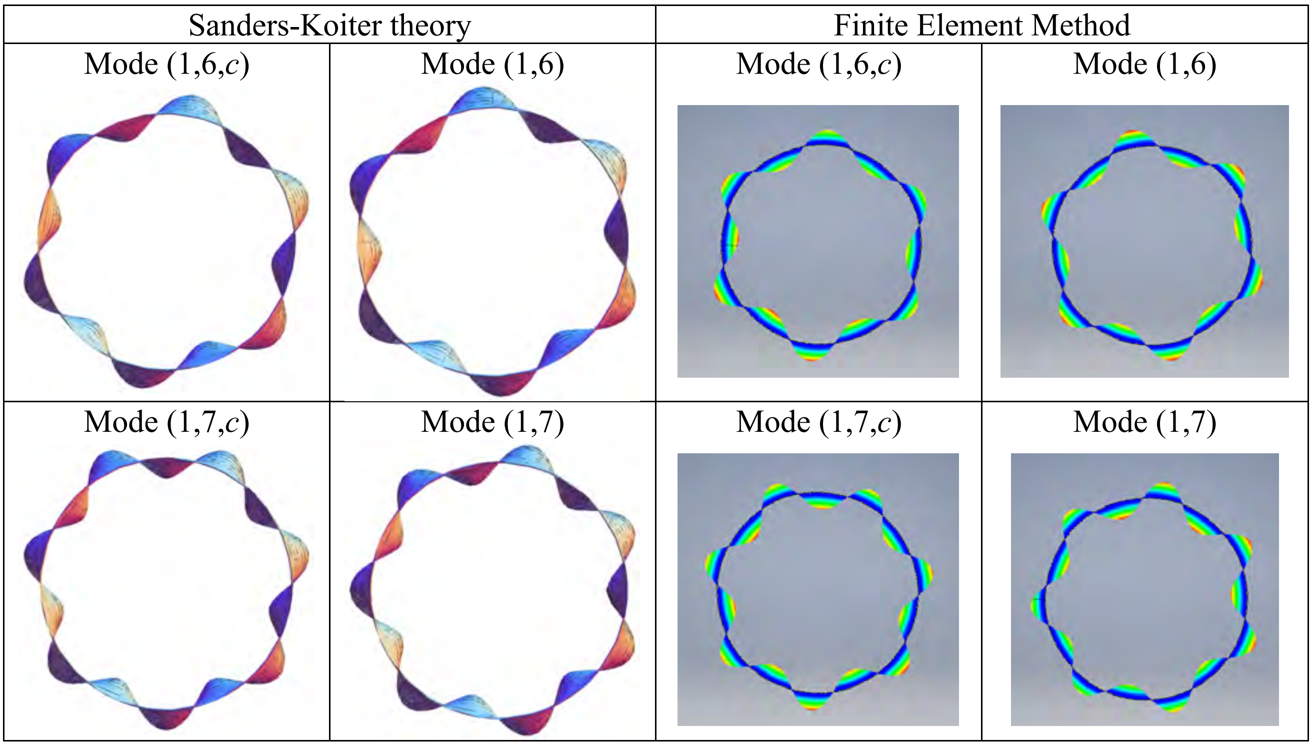

Figure 3: Initial geometric imperfections $wp_{(1,6)} = 0.4h$, $wp_{(1,6,c)} = 0.2h$, $wp_{(1,7)} = wp_{(1,7,c)} = 0$. No localization.

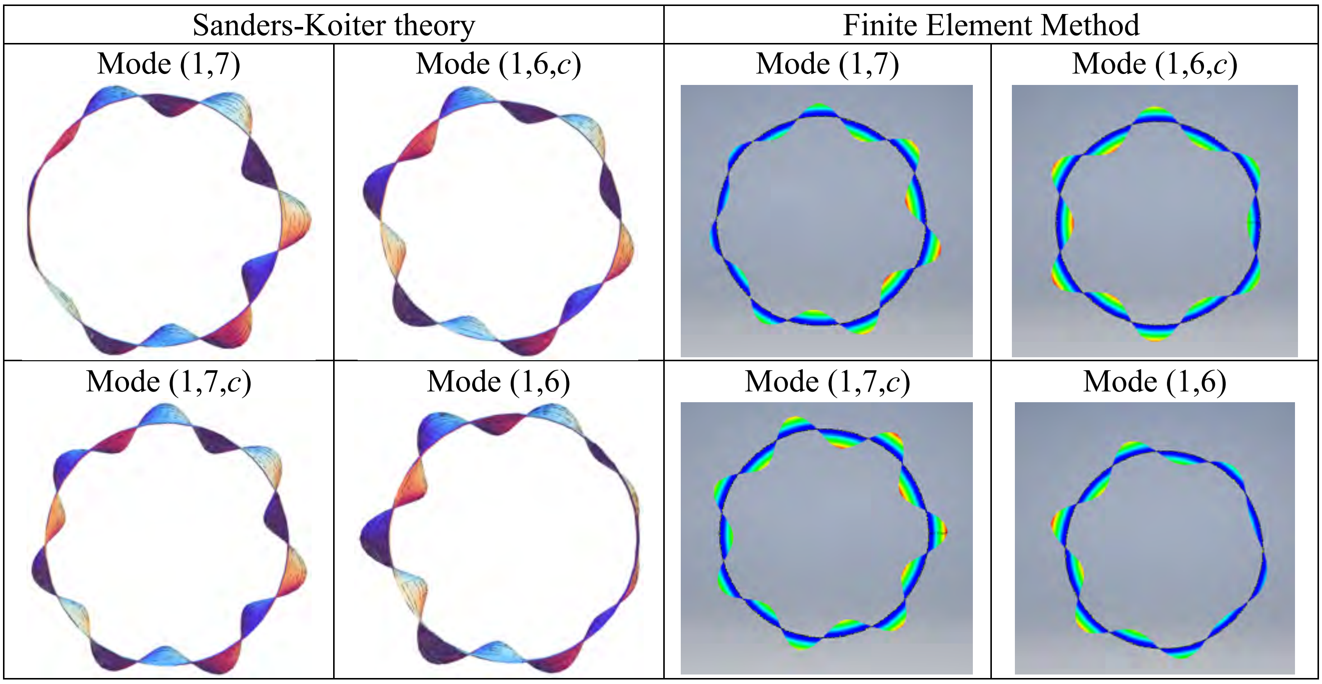

Figure 4: Initial geometric imperfections $wp_{(1,6)} = wp_{(1,7)} = 0.2h$, $wp_{(1,6,c)} = wp_{(1,7,c)} = 0$. Localization.

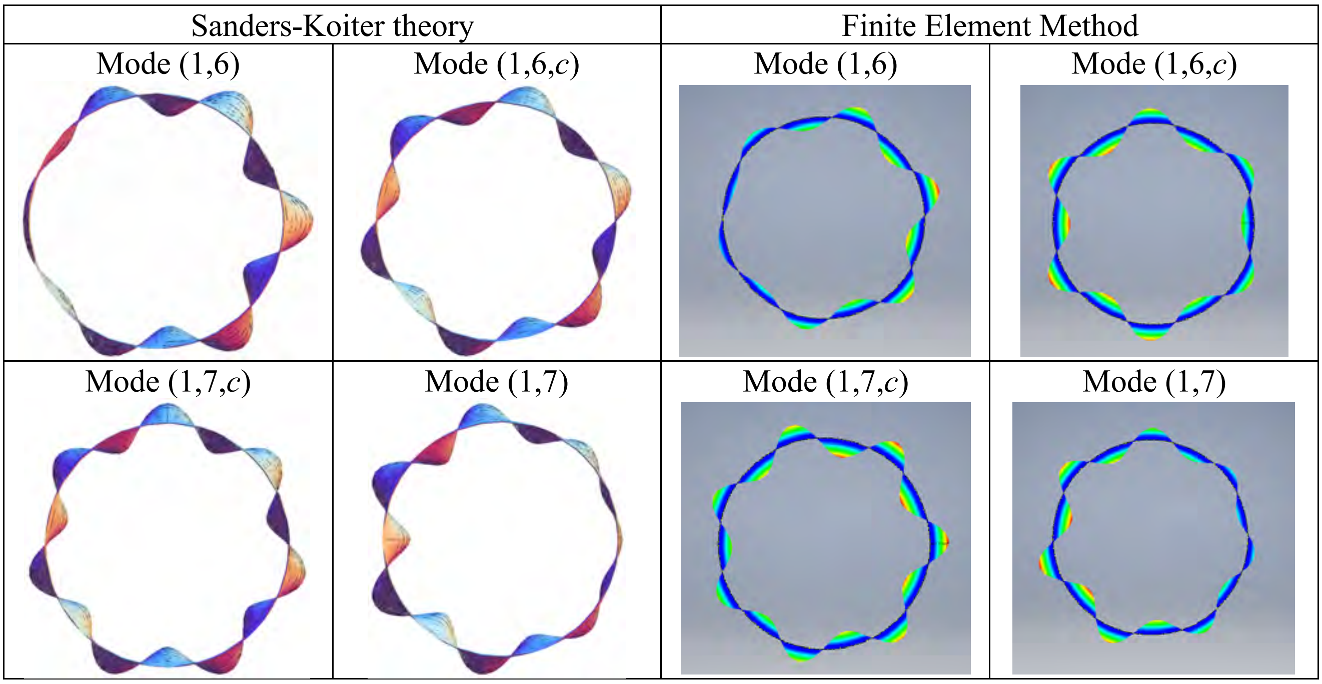

Figure 5: Initial geometric imperfections $wp_{(1,6)} = 0.4h$, $wp_{(1,7)} = 0.2h$, $wp_{(1,6,c)} = wp_{(1,7,c)} = 0$. Localization.

In Figure 4, the initial imperfections considered are $wp_{(1,6)} = wp_{(1,7)} = 0.2h$, $wp_{(1,6,c)} = wp_{(1,7,c)} = 0$: the same initial imperfection imposed on the non-conjugate modes (1,6), (1,7) gives modal localization on all the modes, the localization is maximum on the modes subjected to initial imperfection.

In Figure 5, the initial imperfections used are $wp_{(1,6)} = 0.4h$, $wp_{(1,7)} = 0.2h$, $wp_{(1,6,c)} = wp_{(1,7,c)} = 0$: different initial imperfections imposed on the non-conjugate modes (1,6), (1,7) give modal localization on all the modes, the localization is maximum on the modes subjected to initial imperfection.

Therefore, from Figures 4-5, it can be observed that any initial geometric imperfection imposed on two non-conjugate modes gives localization on the modal shape of all the modes, the localization is maximum on the modal shape of the modes subjected to initial geometric imperfection.

Apparently, the comparison between FEA and semi-analytical model do not match strictly; however, it is to point out that the mode localization is a macroscopic phenomenon caused by a very small perturbation of the geometry, our conjecture is that it is due to a singular perturbation; therefore, it is not surprising that small differences in modelling likely lead to non-negligible differences in the results. More specifically, FEA does not guarantee perfect circumferential continuity like the semi-analytical approach; on the other hand, the latter one is based on series expansion that can suffer of convergence problems.

5. Conclusions

In this paper, the effect of the geometric imperfections on the modal shapes of cylindrical shells is analysed. The Sanders-Koiter shell theory is used. The shell deformation is described in terms of longitudinal, circumferential and radial displacement fields. Clamped-clamped boundary conditions are applied. Geometric imperfections are imposed to investigate the modal localization of the shells.

The semi-analytical approach proposed in this paper is validate in linear field by means of comparisons with finite element analyses. From these comparisons, it is found that any initial geometric imperfection imposed on two conjugate modes gives no localization on the modal shape of all the modes. Conversely, it is seen that any initial geometric imperfection imposed on two non-conjugate modes gives modal localization on all the modes; this localization is maximum on the modal shape of the modes subjected to initial geometric imperfection.

REFERENCES

1 Kubenko, V.D., Koval'chuk, P.S., Influence of initial geometric imperfections on the vibrations and dynamic stability of elastic shells, *International Applied Mechanics*, 40 (8), 847-877, (2004).

2 Watawala, L., Nash, W.A., Influence of initial geometric imperfections on the vibrations of thin circular cylindrical shells, *Computers & Structures* 16 (1), 125-130, (1983). http://dx.doi.org/10.1016/0045.83

3 Shen, H.S., Li Q.S., Thermomechanical post-buckling of shear deformable laminated cylindrical shells with geometric imperfections, *International Journal of Solids and Structures*, 39, 4525-4542, (2002).

4 Byskov, E., Hutchinson, J.W., Mode Interaction in Axially Stiffened Cylindrical Shells, *AIAA Journal*, 15 (7), 941-948, (1977). http://dx.doi.org/10.2514/3.7388

5 Hilburger, M.W., Starnes, J.H., Effects of imperfections of the buckling response of composite shells, *Thin-Walled Structures*, 42, 369-397, (2004). http://dx.doi.org/10.1016/j.tws.2003.09.001

6 Strozzi, M., Pellicano, F., Nonlinear vibrations of functionally graded cylindrical shells, *Thin-Walled Structures*, 67, 63-77, (2013). ISSN: 0263-8231. http://dx.doi.org/10.1016/j.tws.2013.01.009

7 Strozzi, M., Manevitch, L.I., Pellicano, F., Smirnov, V.V., Shepelev, D.S., Low-frequency linear vibrations of single-walled carbon nanotubes: Analytical and numerical models, *Journal of Sound and Vibration*, 333, 2936-2957, (2014). ISSN: 0022-460X. http://dx.doi.org/10.1016/j.jsv.2014.01.016

8 Smirnov, V.V., Manevitch, L.I., Strozzi, M., Pellicano, F., Nonlinear optical vibrations of single-walled carbon nanotubes. 1. Energy exchange and localization of low-frequency oscillations, *Physica D: Nonlinear Phenomena*, 325, 1-12, (2016). ISSN: 0167-2789. http://dx.doi.org/10.1016/j.physd.2016.03.015

9 Pellicano, F., Vibrations of circular cylindrical shells: Theory and experiments, Journal of Sound and Vibration, 303, 154-170, (2007). ISSN: 0022-460X. http://dx.doi.org/10.1016/j.jsv.2007.01.022

10 Strozzi, M., Smirnov, V.V., Manevitch, L.I., Milani, M., Pellicano, F., Nonlinear vibrations and energy exchange of single-walled carbon nanotubes. Circumferential flexural modes, *Journal of Sound and Vibration*, 381, 156-178, (2016). ISSN: 0022-460X. http://dx.doi.org/10.1016/j.jsv.2016.06.013

11 Manevitch, L.I., Smirnov, V.V., Strozzi, M., Pellicano, F., Nonlinear optical vibrations of single-walled carbon nanotubes, *International Journal of Non-Linear Mechanics* (2016). Article in press. ISSN: 0020-7462. http://dx.doi.org/10.1016/j.ijnonlinmec.2016.10.010

12 Pellicano, F., Dynamic stability and sensitivity to geometric imperfections of strongly compressed circular cylindrical shells under dynamic axial loads, *Communications on Nonlinear Sciences and Numerical Simulations*, 14, 3449-3462, (2009). ISSN: 1007-5704. http://dx.doi.org/10.1016/j.cnsns.2009.01.018